Eur. Phys. J. D **42**, 85–91 (2007)
DOI: 10.1140/epjd/e2007-00032-x

THE EUROPEAN PHYSICAL JOURNAL D

Low-energy electron scattering from gaseous CS_2: angular distributions and effect of exchange forces

F.A. Gianturco[1,a] and T. Stoecklin[2]

[1] Department of Chemistry, The University of Rome "La Sapienza" and CNISM, Piazzale A. Moro 5, 00185 Rome, Italy
[2] Laboratoire de Physico-Chimie Moléculaire, 351 cours de la Libération, 33405 Talence, France

Received 23 November 2006
Published online 16 February 2007 –

Abstract. Ab initio calculations are reported for the quantum scattering of electrons from CS_2 molecules in the gas phase and for energies which range from near threshold up to about 100 eV. Angular distributions are examined in detail and an extensive comparison is made with existing experiments and earlier calculations. The agreement found with the latter data is fairly good and results are further discussed in terms of a physical mechanism of "exchange level shifting" to explain the disappearance of a Π_u resonance suggested by earlier studies.

PACS. 34.80.Bm Elastic scattering of electrons by atoms and molecules – 34.80.-i Electron scattering

1 Introduction

The scattering and metastable attachment of low-energy electrons to atomic and molecular targets provide a great variety of interesting phenomena related to fundamental aspects of quantum collisions such as Feshbach resonances [1], virtual state formation [2] or strong energy dependence of the energy transfer efficiency in molecular gases [3].

Among the various systems which have been experimentally analysed to observe the possible presence of any of the above features, together with the comparison with different properties of the elastic cross sections, integral and differential, the carbon disulfide (CS_2) molecular gas has been among the most studied. Together with other linear species with have the same valence electron structures (CO_2 and OCS), it has important applications in laser production studies and in atmospheric chemical processes.

The earliest calculations simply used a model potential [4] within the continuum, multiple scattering approach and examined elastic integral cross sections from 0 to 100 eV: they reported the presence of a shape resonance of Π_u symmetry at 1.85 eV, plus further resonances of different symmetries at higher energies. Additional calculations [5] used the independent atom model to evaluate cross sections for energies above 100 eV, while Lee et al. [6] calculated elastic differential, integral and (elastic+inelastic) cross sections by employing the Schwinger iterative method combined with the distorted wave approximation. Their results showed the presence of a Ramsauer-Townsend (RT) minimum around 0.2 eV but found no indication for the low energy Π_u shape resonance reported earlier [4].

Further calculations [7] of the elastic, integral and differential cross sections were carried out for energies between 5 eV and 50 eV using the Schwinger multichannel method with pseudopotential models within the Static-Exchange (SE) approximation. By using the same method as above, later studies [8] showed that the Π_u resonance present at the SE level of approximation becomes a bound state when polarization effects are included in the scattering calculations.

The corresponding experimental studies have reported, over the years, total, elastic and also vibrationally inelastic cross sections which exhibited a minimum around 0.8 eV [9], while Sohn et al. [10] reported differential and vibrationally inelastic cross sections where they found a minimum around 0.8 eV in the elastic channel: both the above experiments saw no indication of the Π_u resonance surmised by the earlier calculations [4]. More recent measurements [11] analysed collision cross sections below 0.2 eV of energy and detected the presence of giant resonances superimposed on a sharp rise of the cross section that was attributed to the presence of a virtual state for the CS_2^- system. The most recent calculations to date [12] reported a study using the Schwinger multichannel method implemented with pseudopotentials and added polarisation effects to the SE calculations done earlier. Their computed cross sections showed a sharp increase near zero energy followed by an RT minimum around 0.7 eV: they also did not find the presence of the Π_u resonance of earlier studies [4].

[a] e-mail: fa.gianturco@caspur.it

In the present analysis we have therefore decided to revisit the calculations on electron scattering off CS_2 molecules in the gas phase in order to assess once more, using an essentially exact, all-electron SE calculation plus the model treatment of correlation effects via a Density Functional (DFT) formulation of the short-range part of a correlation-polarisation, V_{cp}, interaction potential. The aim was to see in more detail the role of exact exchange forces in either producing or removing the dubious Π_u resonance, to further assess the presence of an RT minimum and of a virtual state and to make a more extensive comparison between measured and computed differential cross sections (DCS).

The following Section 2 briefly outlines our theoretical approach while Section 3 reports the integral cross sections and the resonance behavior. Section 4 shows the comparison of the present DCS values with experiments and earlier calculations, while Section 5 summarizes our conclusions.

2 The theoretical treatment

Within a single-center expansion (SCE) of the continuum wavefunction and of the interaction potential, the use of the Exact-Static-Exchange (ESE) approximation gives rise to a set of coupled integro-differential equations [13]

$$\left\{\frac{d^2}{dr_e^2}+\frac{l(l+1)}{r_e^2}+k^2\right\}u_{ll_0}(r_e)=\sum_{l'}\left\{U_{ll'}(r_e)u_{l'l_0}(r_e)+\sum_{\alpha\beta}\Phi_\alpha^\ell(r_e)W_{\alpha\beta}\int dr\Phi_\beta^\ell(r)u_{l'l_0}(r)\right\} \quad (1)$$

where r describes any of the N-bound electrons and

$$U_{ll'}(r_e)=\int S_l^m(\hat{\mathbf{r}}_e)V(\mathbf{r}_e)S_{l'}^{m'}(\hat{\mathbf{r}}_e)d\hat{\mathbf{r}}_e \quad (2)$$

and

$$\Phi_\alpha^\ell(r_e)=(r_e)\int d\hat{\mathbf{r}}_e\varphi_\alpha(\mathbf{r}_e)S_l^m(\hat{\mathbf{r}}_e) \quad (3)$$

which integrates over real spherical harmonics to yield the radial part of each new function: here the φ_α are the orbitals we shall discuss below. Furthermore

$$S_l^{m,p}(\hat{\mathbf{r}}_e)=\frac{i}{\sqrt{2}}\{Y_l^m(\hat{\mathbf{r}}_e)\pm(-1)^pY_l^{-m}(\hat{\mathbf{r}}_e)\} \quad (4)$$

with the parity index $p=0$ or 1. Here the same equation (3) also holds for the r variable in (1).

One can now express the solution as a linear combination of homogeneous and inhomogeneous terms:

$$u_{ll_0}(r_e)=u_{ll_0}^0(r_e)+\sum_\alpha u_l^\alpha(r_e)C_{l_0}^\alpha \quad (5)$$

where

$$(k^2-H_0^l)u_{ll_0}^0(r_e)=\sum_{l'}U_{ll'}(r_e)u_{l'l_0}(r_e) \quad (6)$$

$$(k^2-H_0^l)u_l^\alpha(r_e)=\sum_{l'}U_{ll'}u_{l'}^\alpha(r_e)+\Phi_\alpha^l(r_e). \quad (7)$$

The coefficients C_l^α are found to satisfy a set of linear equations

$$\sum_\beta A_{\alpha\beta}C_{l_0}^\beta=B_{\alpha l_0} \quad (8)$$

where

$$A_{\alpha\beta}=\delta_{\alpha\beta}-\sum_{l'\gamma}W_{\alpha\gamma}\int\Phi_\gamma^{l'}(r_e)u_{l'}^\beta(r_e)dr_e \quad (9)$$

and

$$B_{\alpha l_0}=\sum_{l'\beta}W_{\alpha\beta}\int_0^0\Phi_\beta^{l'}(r_e)u_{l'l_0}^0(r_e)dr_e. \quad (10)$$

The final numerical integration of the ensuing Volterra equations was then carried out exactly as already described in our previous work [13,14]. If one adopts a one-electron picture for the description of the elastic scattering process in the fixed-nuclei limit, one finds that the collision is determined by an effective Hamiltonian

$$H_{eff}=T+U \quad (11)$$

where T denotes the kinetic energy of the scattered electron and U denotes some optical potential. The latter can be obtained in a variety of ways and its function has often been discussed in the literature [15]. Within the exact static exchange+polarization (ESEP) approximation, the simplest useful approximation to U, one splits it in a local and non-local term, the former being real, energy independent and long ranged while the latter is short ranged and energy-dependent,

$$U(\mathbf{r},\mathbf{r}',E)=V(\mathbf{r})\delta(\mathbf{r}-\mathbf{r}')+W(\mathbf{r},\mathbf{r}',E). \quad (12)$$

All the nuclear coordinates are not explicitly indicated and are supposed to be fixed at their equilibrium values (the FN approximation).

In the present case, the distances adopted were initially those of the molecular equilibrium geometry: $R_{CS}=2.9376a_0$ and the basis set expansion chosen for the target Molecular Orbitals (MO's) was the Valence Double Zeta D95V* [16]. Whenever the scattering process could take place with an 'undistorted' molecular charge distribution and the polarization-correlation effects could be disregarded, then the local potential V becomes the static interaction:

$$V(\mathbf{r}_e)=2\sum_j\int d\mathbf{r}\frac{|\varphi_j(\mathbf{r})|^2}{\mathbf{r}-\mathbf{r}_e}-\sum_k\frac{Z_k}{|\mathbf{r}-\mathbf{R}_k|} \quad (13)$$

and W becomes the exchange interaction without any dependence on the projectile relative energy

$$W(\mathbf{r},\mathbf{r}_e,E)=-\sum_j\frac{\varphi_j(\mathbf{r})\varphi_j(\mathbf{r}_e)}{|\mathbf{r}-\mathbf{r}_e|}. \quad (14)$$

$\mathbf{r}_e$ is now the coordinate of the scattered electron and $\mathbf{r}$ represents the coordinate of a bound electron. In the above equations $\{\phi_j\}$ denotes the set of doubly occupied

self-consistent-field (SCF) orbitals, while $\{R_k\}$ and $\{Z_k\}$ denote the sets of nuclear positions and charges, respectively.

The first step is therefore that of solving the scattering problem for the local and long range potential V. This will be done, as mentioned below, by solving coupled integral equations by a finite-step method. The residual scattering due to the non-local interaction could be done within the T-matrix expansion approach since, due to the short-range character of the exchange potential, W can be quite well represented via the use of a separable approximation [17,18]. Thus we start by approximating the exchange potential W by the truncated separable form:

$$W(\mathbf{r},\mathbf{r}_e) \approx \sum_{\alpha,\beta}^{N} \chi_\alpha(\mathbf{r}) W_{\alpha,\beta} \chi_\beta(\mathbf{r}_e) \tag{15}$$

where the $\{\chi\}$ are now additional, new Cartesian Gaussian functions not necessarily orthogonal to each other, nor to the occupied molecular orbitals to the target SCF basis set mentioned before. We shall describe them in the next section.

The exchange matrix elements for the bound orbitals of the molecule are given by first calculating the following matrix elements

$$\tilde{K}_{\gamma\tau} = \int d\mathbf{r} \int d\mathbf{r}_e \varphi_\gamma(\mathbf{r}) W(\mathbf{r},\mathbf{r}_e) \varphi_\tau(\mathbf{r}_e) \tag{16}$$

hence

$$\tilde{K}_{\gamma\tau} = \sum_{\alpha,\beta} \int d\mathbf{r} \varphi_\gamma(\mathbf{r}) \chi_\alpha(\mathbf{r}) W_{\alpha,\beta} \int d\mathbf{r}_e \varphi_\tau(\mathbf{r}_e) \chi_\beta(\mathbf{r}_e) \tag{17}$$

and

$$\tilde{K}_{\gamma\tau} = \sum_{\alpha,\beta} S_{\gamma\alpha} W_{\alpha,\beta} S_{\beta\tau} \tag{18}$$

we are finally looking for the exchange matrix $\mathbf{W}$ as given by

$$\mathbf{W} = \mathbf{S}^{-1} \tilde{\mathbf{K}} \mathbf{S}^{-1} \tag{19}$$

with $S_{\alpha\beta}$ being the overlap matrix elements.

We obtain a quadrupole moment $Q = 2.325$ au in good agreement with the experimental value. The analytical coefficients for the expansion of each occupied molecular orbital ϕ_i were given, in symmetrized, real spherical harmonics, with l values up to 200, as

$$\phi_i^m(\mathbf{r}) = \sum_l C_l^m(r) S_l^{m,p}(\theta,\phi). \tag{20}$$

The above expansion was then used to generate the electrostatic potential:

$$V(r) = \int d\mathbf{r}' \sum_i \frac{\phi_i^m(\mathbf{r}) \phi_i^{m*}(\mathbf{r}')}{|\mathbf{r}-\mathbf{r}'|} \tag{21}$$

and the potential was finally expanded in Legendre polynomials up to $l = 80$ for the maximum multipolar coefficient.

Table 1. Separable exchange GTO's employed in the calculations.

Σ_g symmetry
(a) on the C atom
s: 20.0; 9.0; 5.0; 3.0; 1.7; 1.0; 0.6; 0.35; 0.2, 0.1
dzz: 8.0; 4.0; 2.0; 1.0; 0.5; 0.25; 0.1
(b) on the S atom
s: 8.0; 4.0; 2.0; 1.0; 0.5; 0.25, 0.1
pz: 8.0; 4.0; 2.0; 1.0; 0.5; 0.25; 0.1
dzz: 8.0, 4.0; 2.0; 1.0; 0.5; 0.25; 0.1
Σ_u symmetry
(a) on the C atom
s: 20.0; 9.0; 5.0; 3.0; 1.7; 1.0; 0.5; 0.25; 0.12; 0.08
dzz: 16.0; 8.0; 4.0; 2.0; 1.0; 0.5; 0.25; 0.12; 0.08
(b) on the S atom
pz: 16.0; 8.0; 4.0; 2.0; 1.0; 0.5; 0.25; 0.12; 0.8
dzz: 16.0; 8.0; 4.0; 2.0; 1.0; 0.5; 0.25; 0.12; 0.08
Π_g symmetry
(a) on the C atom
dxz: 20.0; 9.0; 5.0; 3.0; 1.7; 1.0; 0.6; 0.35; 0.2; 0.12
(b) on the S atom
px: 64.0; 32.0; 16.0; 8.0; 4.0; 2.0; 1.0; 0.5; 0.25; 0.1
dxz: 16.0; 8.0; 4.0; 2.0; 1.0; 0.5; 0.25; 0.1
Π_u Symmetry
(a) on C atom
px:20.0; 9.0; 5.0 3.0; 1.7; 1.0; 0.6; 0.35; 0.2; 0.12
(b) on the S atom
px: 64.0; 32.0; 16.0; 8.0; 4.0; 2.0; 1.0; 0.5; 0.25; 0.1
dxz: 16.0; 8.0; 4.0; 2.0; 1.0; 0.5; 0.25; 0.1
Δ_g symmetry
(a) on the C atom
dxx:20.0; 9.0; 5.0; 3.0; 1.7; 1.0; 0.6; 0.35; 0.2; 0.12
(b) on the S atom
dxx: 16.0; 8.0; 4.0; 2.0; 1.0; 0.5; 0.25; 0.1
fx2z: 16.0; 8.0; 4.0; 2.0; 1.0; 0.5; 0.25; 0.1
Δ_u symmetry
(a) on the C atom
fx2z: 20.0; 9.0; 5.0; 3.0; 1.7; 1.0; 0.6; 0.35; 0.2, 0.12
(b) on the S atom
dxx: 16.0; 8.0, 4.0; 2.0; 1.0; 0.5; 0.25; 0.1
fx2z: 16.0; 8.0, 4.0; 2.0; 1.0; 0.5; 0.25; 0.1

2.1 The polarization potential

As mentioned in the introduction we used in the inner region the density functional form as given by Padial and Norcross [19]. The asymptotic part of this potential was calculated using the experimental values of the polarization: $\alpha_0 = 55.4a_0^3$; $\alpha_2 = 39.14a_0^3$.

2.2 The exchange potential

The Gaussian basis set $|\gamma_\alpha\rangle$ that we used to expand the exchange kernel for the 19 occupied MO's is given for each symmetry in Table 1 where the meaning of the symbols is explained there.

The expansion of the orthogonalized basis set in spherical harmonics was carried out analytically by using the shifting of Gaussian functions and we took for each type

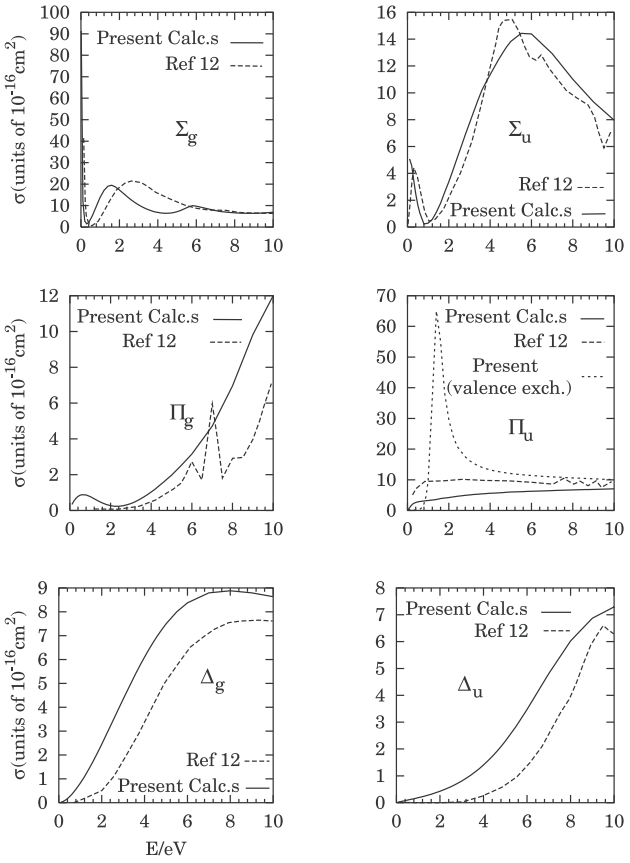

Fig. 1. Computed partial integral elastic (rotationally summed) cross sections, as a function of collision energy, for all contributing symmetry components. Solid line: present results; dashed lines: calculations from reference [12]. Short dashes: our calculations with only valence orbitals included in the exchange (Π_u component).

of basis functions the first two contributions to this expansion. The l values went up to $l_{max} = 28$ for Σ orbitals, up to 15 for Π orbitals and Δ orbitals. The steps of the grid for the radial coordinate were taken to be $0.005a_0$ up to $R = 10a_0$. For larger values of R, and up to distances of $500a_0$, we employed the asymptotic part of the static potential plus the polarisation potential indicate above.

The partial waves employed in the scattering calculations went up to $l_{max} = 60$ for the scattered electron when the index of the multipolar coefficients went up to 100. For multipolar terms in the potential beyond $l = 80$ we only employed the asymptotic part of the static interaction of equation (21). Convergence was checked against all the above parameters and the size of the basis set expansion: all reported quantities are converged within the third significant figure.

3 Results and discussion

3.1 Integral cross sections

In order to assess the quality of the present calculations, we report in Figure 1 the behavior of the individual partial

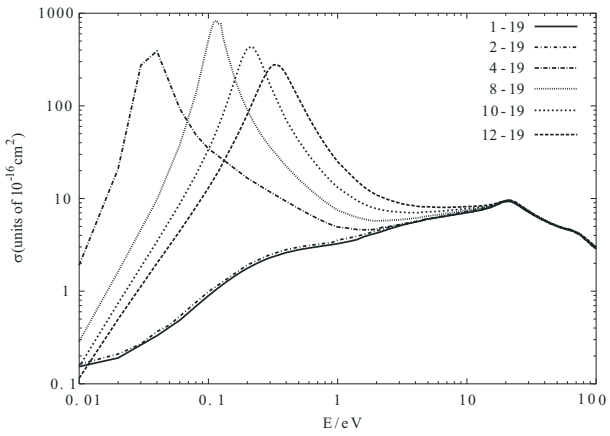

Fig. 2. Computed integral partial cross sections of Π_u symmetry as a function of the number of bound orbitals included in the description of the exchange potential. The curve marked by crosses corresponds to that given by a solid line in Figure 1.

cross sections contributing for each symmetry component as a function of collision energy, from threshold and up to 10 eV.

The results are shown for the six different symmetries which contribute to the total cross sections over that range of energy. The dashes report the same calculations from the recent work on Bettega et al. [12]. The following comments could be made:

1. in spite of the differences in methodology and on the numerical treatment of the interaction forces, it is reassuring to see that our present results follow fairly closely the recent data of reference [12];
2. the Π_u resonance surmised by earlier studies [4] is not present in our results (solid line) nor in the recent calculations (dashes). We see, however, that if we artificially eliminate the correlation-polarization contribution to the scattering process (short dashes) by weakening the attractive interaction, this causes one of the bound states in the Π_u symmetry to become a resonant state: the latter, however, disappears when the correct (stronger) interaction forces are employed. The effect on the scattering when the exchange contributions are gradually included could be better analysed by looking at the results of our numerical experiment reported by Figure 2. The calculations shown there indicate the changes in the Π_u component of the cross sections as the number of bound orbitals contributing to the exchange kernel is varied: one clearly sees there that only the inclusion of all the target MO's (curve with crosses) in describing the full exchange is able to bring the scattering electron down to occupying a bound state of the target, thereby eliminating the spurious resonant features shown when an artificially weaker interaction is employed in the calculations. In other words, even if the correlation-polarization terms are included in the full interaction, the behavior of the Π_u component still shows the presence of a resonant state whenever the exchange contribution is made weaker than its correct value. Thus, the full inclusion

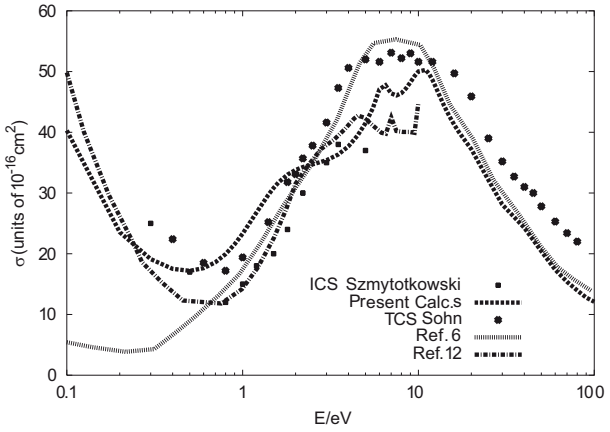

Fig. 3. Computed and measured total integral cross sections from threshold and up to 100 eV. Solid line: present results; dot-dashes: calculations from reference [12]; dots: calculations from reference [6]. Filled-in squares: expt.s from reference [10]; filled-in circles: expt.s from reference [9].

of exchange effects (which were only qualitatively modeled in the calculations of [4]) is an essential ingredient for transforming a spurious resonance in a many-electron system into an additional bound state, this being the case even if the V_{cp} interaction is included.

All sets of calculations given by Figure 3 indicate regions where partial maxima should appear in the total cross sections and also show the presence of a Ramsauer-Townsend (RT) minimum below 1 eV of collision energy, as also indicated by the Σ_g and Σ_u contributions shown in Figure 1. The comparison with the available data for the total elastic cross sections is also given in Figure 3, where the following considerations could be made from analysing such data:

1. our computations follow rather closely the experiment of Sohn et al. [10] and indicate the same presence of a couple of resonant features from 6 to 10 eV, albeit less broadened than in the experiments;
2. our RT feature is also clearly present and seems to appear slightly below the 0.8 eV location of the experiments: we see it around 0.6 eV. Only one of the earlier calculations, the dot-dashes from reference [12] confirm the minimum feature and gives it closer to the experimental findings;
3. the overall size of the computed cross sections follows rather nicely the experimental energy dependence and is also in line with the earlier computations reported in the figure.

3.2 Angular distributions

Another important test when assessing the the quality of calculations is that provided by a comparison of the computed differential cross sections (DCSs) with either earlier computations or existing experiments. In the following figures (Figs. 4–7 we report such a comparison for the results concerning our title system.

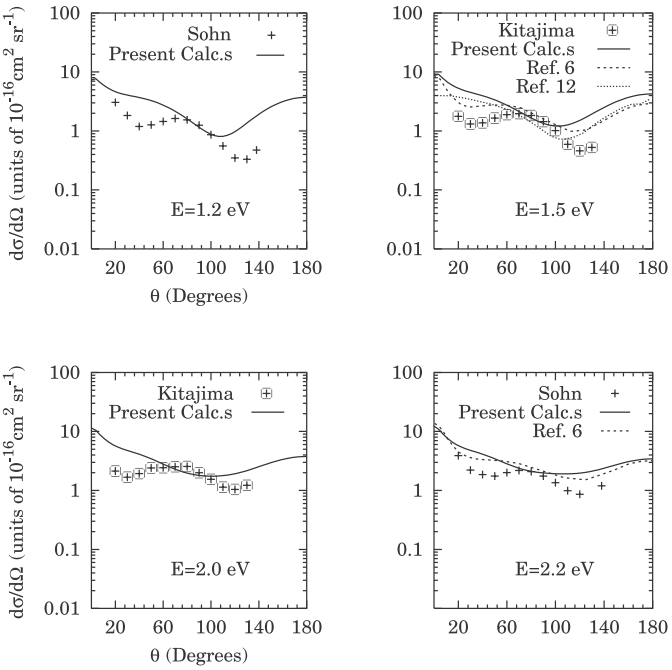

Fig. 4. Computed and measured angular distributions in the low energy domain: the experiments are: (+) from reference [10] and (⊞) from reference [20]. Our calculations are given by a solid line, while the dashes refer to the calculations of reference [6] and the dots to calculations from reference [12].

The lower energy behavior of the angular distribution is shown by Figure 4, where both experiments and calculations are given in absolute units and are seen to be very close to each other in terms of relative sizes. Furthermore, we see that our present data are essentially coincident with the earlier calculations of [6,12] and also give rather well the general shape of the measured quantities.

When we look at the next energy range from 3.0 to 5.0 eV, we see that the present results are doing well in reproducing the experimental data: a more marked forward scattering feature in the measurements is also clearly given by our calculations. Furthermore, the existing earlier computations, in spite of coming from an entirely different treatment of the scattering process, are seen to be very close to the present results.

If we now move to a still higher energy domain which goes from 8.0 eV up to 20.0 eV (see results of Fig. 6), we see again a very nice agreement between calculations and experiments: our results indicate an increase in size of the cross sections as the scattering moves to the backward region, although the experiments have no data beyond 130° to confirm this behavior. The earlier calculations, whenever available are also very close to the present ones.

The highest energies available experimentally are studied in the three panels of Figure 7, where we also compare our calculations with experiments and with other, earlier computations [6].

Considering the complexity of the calculations, we see that the existing experiments are once more well

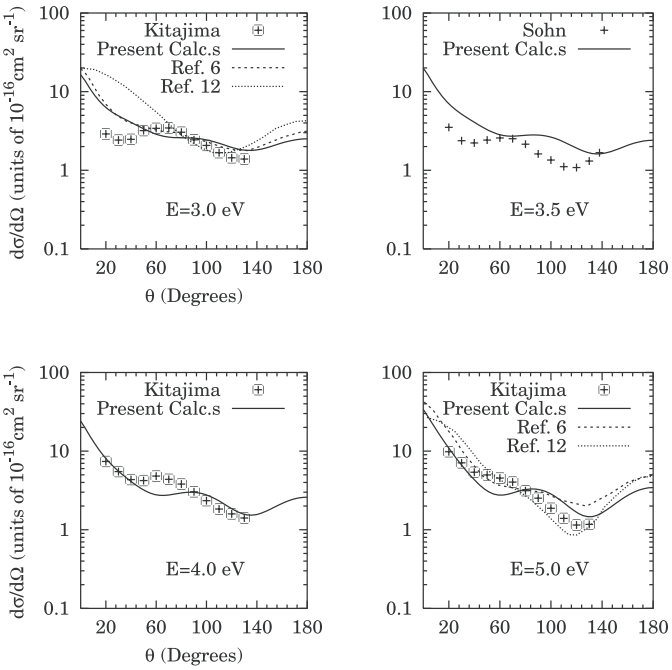

Fig. 5. Same quantities as in Figure 4 but for an higher energy range from 3.0 to 5.0 eV. See text for details.

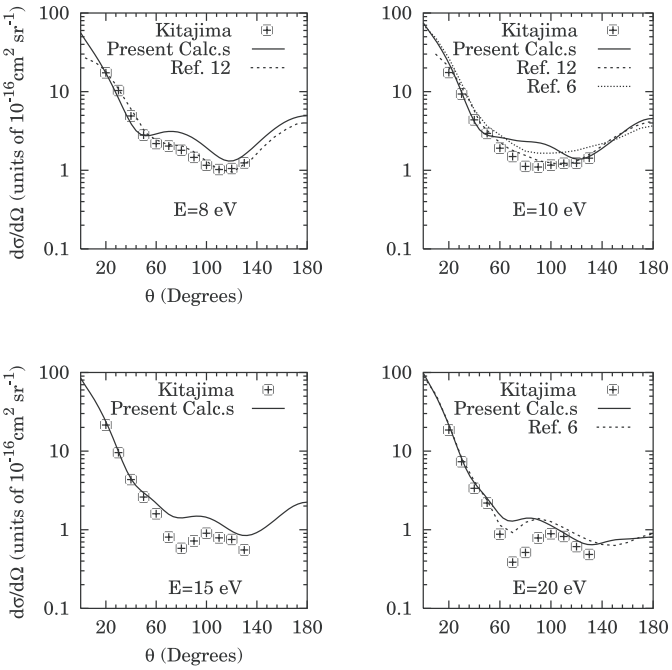

Fig. 6. Same quantities as in Figure 4 but for the higher energy domain from 8.0 to 20.0 eV. See main text for details.

reproduced by the present data which, at 100 eV, are also fairly close to the only existing earlier calculations [6].

Another useful piece of information is reported by the results of Figure 8, where we compare the integral cross sections of Figure 3 with the momentum transfer cross sections (MTCS) as obtained from the previous angular

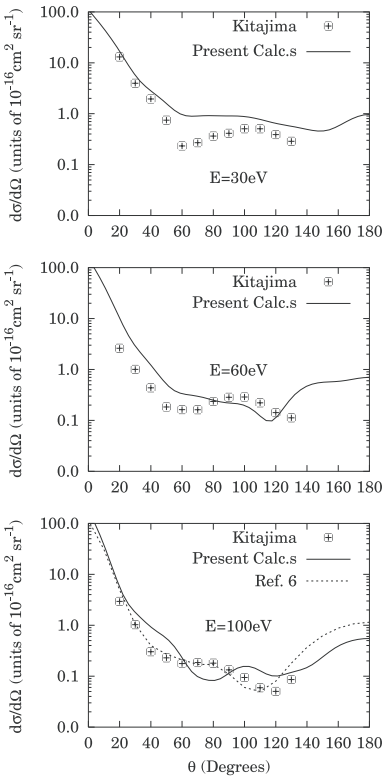

Fig. 7. Same quantities as in Figure 4 but for the highest energies considered in this work. See there for details on the symbols used.

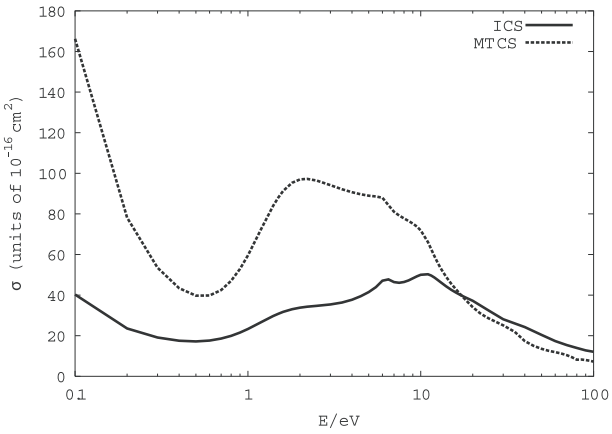

Fig. 8. Computed integral cross sections (ICS) and momentum transfer sections (MTCS) from threshold up to 100 eV.

distributions by the following integration

$$\sigma_{MT}(k^2) = 2\pi \int \frac{d\sigma}{d\Omega}(k^2)(1-\cos\vartheta)d\vartheta. \qquad (22)$$

The comparison with the ICS given in the figure clearly indicates the strong backward scattering effects which appear as the collision energy decreases and which cause a strong surge of the MTCS below 0.5 eV. Furthermore, we see the broad region of large values of the MTCS between 1 and 10 eV, associated again with strong backward scattering in that energy range as visible from the computed

DCS discussed before. On the other hand, as the collision energy increases towards 100 eV, the angular distributions favor the forward scattering region, as shown by our data in Figures 5 to 7. Hence, the corresponding MTCS values decrease monotonically and follow the ICS size and behavior in that region.

It is also interesting to note that an earlier study on e^--CS_2 scattering [21] showed from calculations that the lowest energy geometry for CS_2 was a bent structure and that a linear transition state exists very close in energy and with a geometry very close to that of neutral CS_2. Further experimental studies on CS_2 resonant behavior [22] suggested the formation of CS_2^- around 15 meV and a giant resonance associated with a bent CS_2^- around 49 and 82 meV attributed to virtual state formation.

Our present calculations indicate indeed the presence of a negative scattering length ($A_0 = -3.70a_0$) for the equilibrium geometry and a corresponding energy location of a virtual state around 0.9 eV, not far from the RT feature shown by Figures 1, 2 and 3 and from the virtual state formation invoked for the intermediate structure of the metastable anion by [21,22].

Furthermore, we have found in our calculations of the scattering length as a function of bond length that its values become markedly larger (i.e. the virtual state energy location moves closer to a zero-energy resonance position) as the bond is symmetrically stretched: for $R_{cs} = 2.35$ Å we get, in fact, an A_0 value of $-6.74a_0$, and for R_{cs} further stretched to 3.23 Å we obtain: $A_0 = -12.49a_0$. Thus, we can surmise that geometry deformations (symmetric stretching in our numerical experiment) can lead to a virtual state evolution into a zero-energy resonance which could then be responsible for the giant features observed by the experiments of [22].

4 Present conclusions

The calculations described in this work have analyzed the nanoscopic origin of the spurious Π_u resonance reported earlier for CS_2 and have shown that, in a multi-electron target like this molecule, the correct treatment of exchange forces is an important ingredient for realistically describing the attractive features of the overall interaction: by reducing the number of bound electrons involved in the exchange with the scattering electron, in fact, we have shown that a spurious resonant state fails to become a bound state of the anionic system and therefore artificially modifies the energy behavior of the Π_u component of the total ICS.

By further using the full exchange contribution we have computed the low energy RT feature and found it to occur around 0.6 eV, in fair agreement with experiments. The angular distributions have also been computed over a very broad range of collision energies and turned out to agree reasonably well with the existing experiments and with earlier calculations.

Finally, the use of the Modified Effective Range Theory (MERT) [23] in calculating the s-wave scattering length reveals the presence of a virtual state around 0.9 eV when the molecule is considered in its equilibrium geometry, a feature connected with the existence of the RT minimum. It further suggests that molecular deformations (bond stretching) cause the virtual state energy location to move closer to the zero-energy line and therefore to acquire the features of a resonance that, in keeping with the experimental observation [22], can in turn cause a dramatic change in the energy dependence of the ICS at very low collision energies.

The financial support of the Italian Ministry for University and Research (MUIR), of the CASPUR Supercomputing Consortium and of the Research Committee of the University of Rome "La Sapienza" is gratefully acknowledged. We also thank the EIPAM program of the ESF for financing visits to Rome by T.S. while this work was completed. We finally thank professor Tanaka for sending us the relevant experimental DCS which we used in our comparison with the present calculations.

References

1. E. Leber, S. Barsotti, J. Bommels, J.M. Weber, I.I. Fabrikant, M.-W. Ruf, H. Hotop, Chem. Phys. Lett. **325**, 345 (2000)
2. D. Field, N.C. Jones, S.L. Lunt, J.-P. Ziesel, Phys. Rev. A **64**, 22708 (2001)
3. S. Telega, F.A. Gianturco, Eur. Phys. J. D **38**, 495 (2006)
4. M.G. Lynch, D. Dill, J. Siegel, J.L. Dehmer, J. Chem. Phys. **71**, 4249 (1979)
5. D. Ray, S. Tomar, J. Phys. B **30**, 1989 (1997)
6. M.T. Lee, S.E. Michelin, T. Krain, E. Veitenheimer, J. Phys. B **32**, 3043 (1999)
7. M.H.F. Bettega, A.P.P. Natalense, M.A.P. Lima, L.G. Ferreira, Braz. J. Phys. **30**, 189 (2000)
8. M.H.F. Bettega, Aust. J. Phys. **53**, 785 (2000)
9. Cz. Szmytkowski, J. Phys. B **20**, 6613 (1987)
10. W. Sohn, K.-H. Kochem, K.-M. Schauerlein, K. Jung, H. Ehrahrdt, J. Phys. B **20**, 3217 (1987)
11. N.C. Jones, D. Field, J.-P. Ziesel, D.A. Field, Phys. Rev. Lett. **89**, 093201 (2002)
12. M.H.F. Bettega, M.A.P. Lima, L.G. Ferreira, J. Phys. B **38**, 2087 (2005)
13. F.A. Gianturco, T. Stoecklin, J. Phys. B **27**, 5903 (1994)
14. A. Jain, D.W. Norcross, Phys. Rev. A **32**, 1341 (1985)
15. E.g. see: J.S. Bell, E.J. Squires, Phys. Rev. Lett. **3**, 205 (1977)
16. T.H. Dunning Jr, P.J. Hay, *Modern Theoretical Chemistry*, edited by H.F. Schaefer III (Plenum Publ. Co., New York, 1976), Vol. 3
17. T.M. Rescigno, A.E. Orel, Phys. Rev. A **24**, 1267 (1981)
18. T.M. Rescigno, A.E. Orel, Phys. Rev. A **25**, 2402 (1982)
19. N.T. Padial, D.W. Norcross, Phys. Rev. A **29**, 1590 (1984)
20. M. Tanaka, private communication
21. G. Gutsev, R.J. Bartlett, R.N. Compton, J. Chem. Phys. **108**, 6756 (1998)
22. N.C. Jones, D. Field, J.-P. Ziesel, T.A. Field, Phys. Rev. Lett. **89**, 093201 (2002)
23. E.g. see R.G. Newton, *Scattering Theory of Waves amd Particles* (Springer-Verlag, New York, 1992)